Available on CMS information server

CMS NOTE 1998/011

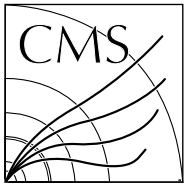

The Compact Muon Solenoid Experiment

CMS Note

Mailing address: CMS CERN, CH-1211 GENEVA 23, Switzerland

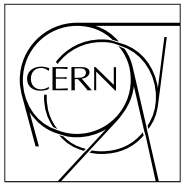

11 February 1998

Temperature dependence of the behaviour of a single-sided irradiated silicon detector

E. Babucci, P. Bartalini, G.M. Bilei, S. Bizzaglia, B. Checcucci, P. Lariccia, G. Mantovani, A. Santocchia, L. Servoli, Y. Wang

INFN and Perugia University, Italy

N. Dinu, V. Postolache

Buchuresti University, Rumania

Abstract

We have studied the behaviour of a single-sided, 50 μm pitch, AC-coupled, poly-resistor biased silicon detector, processed at CSEM (Neuchatel, Switzerland) after having been irradiated with a fluence of 1×10^{13} neutrons/cm^2. The irradiation has been performed simulating the CMS silicon tracker data taking environment, with the detectors under bias and the temperature at 0 ^oC. During the july 1996 test beam period we tested the detector at different temperatures (-10,-5,0,+5,+20 ^oC) as a function of the bias voltage up to 200 V, with the 120 GeV pion beam of X7 area at CERN. On these conditions we measured a S/N ratio $\sim$ 12-14, efficiency $\sim$ 98-99 % and a spatial resolution $\sim$ 11-13 μm.

1 Introduction

The tracking system of the CMS experiment [1] will be exposed to high radiation doses at the LHC proton-proton collider. Among the components of the tracker, the silicon detectors will undergo type inversion after a period of time from the beginning of the LHC starting phase. This work concentrates on the temperature dependence of the working characteristics of a prototype silicon detector, irradiated until type inversion and then tested under the same conditions that will be present during the running of LHC.

2 The Detector and the irradiation procedure

We have used a single-sided silicon detector (CMS01) fabricated by CSEM with the standard p^+n technology. The detector lenght was 6.22 cm, the thickness 300 μm, the interstrip pitch 50 μm and there were 384 strips. Before irradiation the detector had a depletion voltage of 27 V and a leakage current of 170 nA.

The detector has been irradiated at the ENEA facility [2] in Casaccia (Roma), with a fluence of 1×10^{13} neutrons/cm^2, with an energy spectrum very similar to the one present at LHC, under bias (40 V) and at a temperature of 1 ± 1 ^oC, simulating thus the running environment of the CMS silicon tracker.

After the irradiation the depletion voltage has been measured to be 21 V, in agreement with expectations [3], and the leakage current 0.17 mA. The irradiation damage constant α has been computed and the result is α = (4.2 $\pm$0.8)$\times10^{-17}$ A/cm (at 25 V) in agreement with what was expected [4, 5].

The detector was then mounted on a mechanical support and connected to an array of PREMUX128 chips [6] reading out every strip. All strips have been read out. The assembled module (SS) has then been kept at 0 ^oC.

3 The experimental setup and the data acquisition

The beam test was performed in july 1996 in the X7 beam line of the CERN SPS West Area, with a pion beam of 120 GeV energy. The schematic setup is shown in fig. 1.

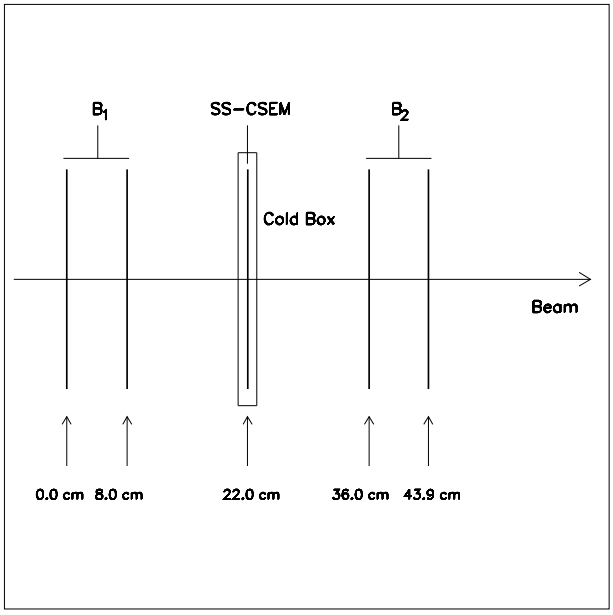

Figure 1: Test Beam setup during july 1996 tests.

The module was inserted in a cold box, where the temperature could be varied from -20 ^oC up to room temperature, and then installed between the 4 double-sided silicon planes, B_1 and B_2, that were part of the telescope [8].

We could hence reconstruct the track of the incident pion and then predict very precisely the position of the impact point on the single-sided silicon detector, for both coordinates.

A description of the data acquisition system can be found in [9]. We performed a scan in temperature (-10, -5, 0, +5, +20 ^oC) and in bias voltage (+15 to +200 V), taking about 10K triggers per each point of the scan.

4 Data analysis

The data have been analized using the TT5 package [10], developed by the Aleph/CMS collaboration, both for the detectors of the telescope than for the one under test. The most important parameters of the algorithm used to select a cluster are summarized in table 1 where units of σ_{noise} are used.

Table 1: Main cuts to define a cluster.

Parameters Set Optimized for:	Central Strip Cut	Neighbor Strips Cut	Cluster Cut
Telescope (typical)	5.0	4.0	7.0
SS	4.0	3.0	3.0

The first row defines the typical value of the cuts that were choosen to analize the telescope data; for each instrumented plane we find all clusters that survive the cuts, and then we preserve the cluster with the highest collected charge, discarding the others.

The telescope planes have been aligned using the same procedure of the 1995 CMS tracker test beam [9]. The extrapolation error on the impact point (estimated from the errors on the points measures by the telescope planes) has an average value of 5.5 μm.

We applied some cuts to select events with good track reconstruction:

- 4 points found by the telescope in the coordinate measured by the test detector, and at least 2 points in the other coordinate;
- the extrapolated point should fall inside a fiducial region of the test detector where there are no dead channels due to known bonding problems;
- a small extrapolation error on the impact point on the test detector (< 20 μm).

We then searched clusters in the test device using the second row of table 1, where the parameters have been optimized to maximize the efficiency of the detector.

4.1 Basic detector performances

If we choose a working point (-5 $^oC$and $+150\,V$) where the detector is fully depleted, then:

- The cluster noise (fig. 2) is centered around a value of 8.4 ADC counts, somewhat higher with respect to our expectations, but still manageable. The reason for the high value of the noise is to be found outside the detector; in fig. 3 we plot the noise of the dead (unconnected) channels that clusters around a value of 5.5 ADC counts, more than twice the expected value, leaving only a value of 2.9 ADC counts as the contribution of the silicon detector and the capacitive load of the preamplifier. From the general noise formula adapted [6, 7] to the PREMUX128 chip and to our detector, we would have expected that the unconnected channels would contribute for 45% of the total noise, while we have in our case 65%.
- The cluster size (fig. 4) has a reasonable shape and average value ($\sim$1.5).
- The cluster charge (fig. 5) is well fitted by a Landau distribution, and peaks at 118 ADC counts; we can also see the contribution of the different type of clusters, according to their size: one, two or more strips.
- The signal/noise distribution obtained event by event as the ratio between the cluster charge and the cluster noise is reported in fig. 6; we notice that the most probable value 13.8, is compatible with the usual way of defining the signal/noise as the ratio among the most probable values of the Landau distribution of fig. 4

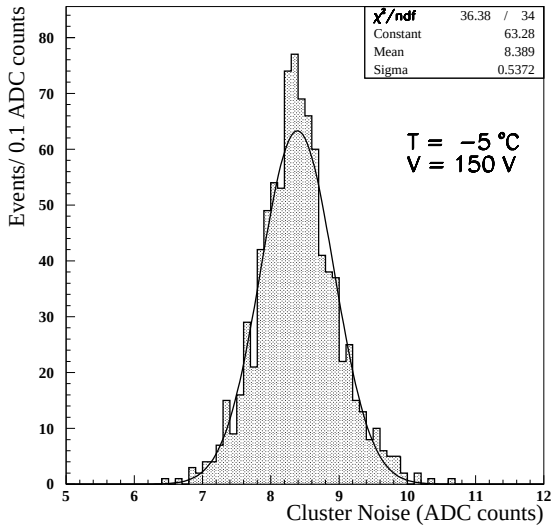

Figure 2: Cluster Noise distribution

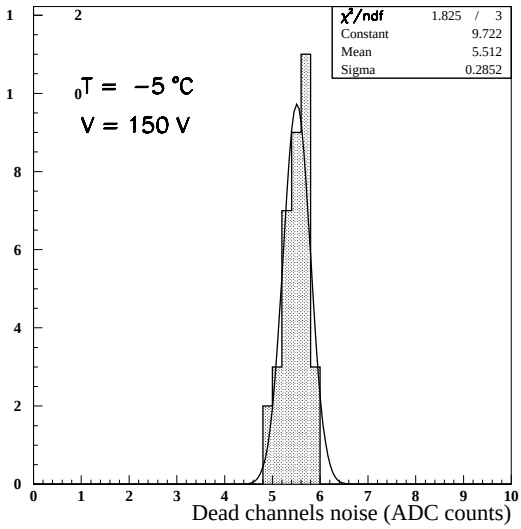

Figure 3: Cluster Noise for unconnected channels

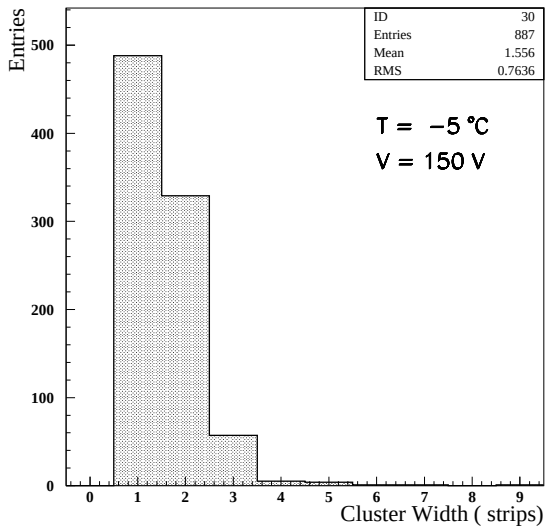

Figure 4: Cluster Width distribution

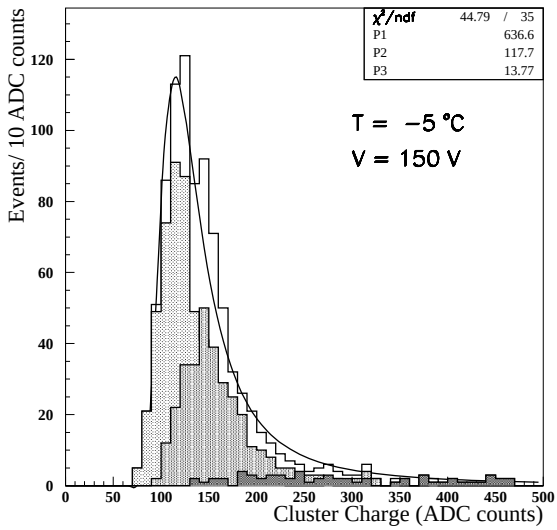

Figure 5: Cluster charge distribution for a) all clusters (empty area); b) one strip clusters (gray area); c) two strips clusters (vertical bar area); d) three strips clusters (black area);

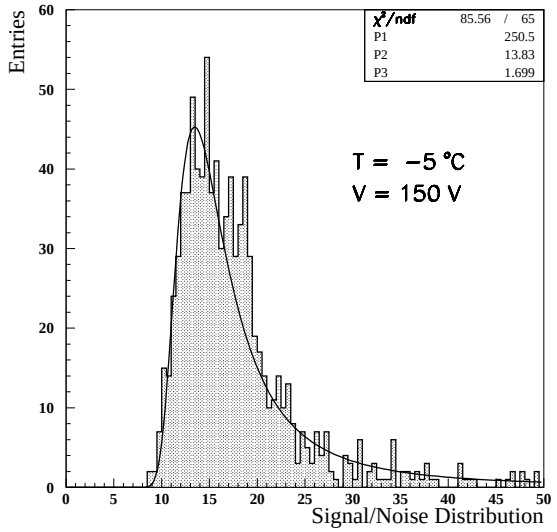

Figure 6: Signal/Noise distribution event by event.

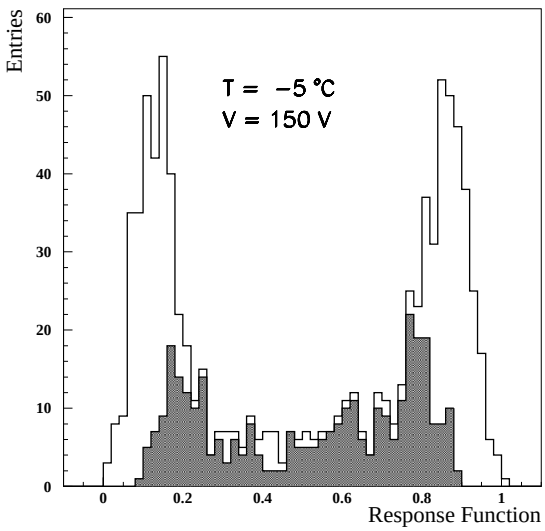

Figure 7: Response Function for a) all clusters (empty area) b) two strips clusters (black area).

and the one of the gaussian distribution of fig. 3, that, in this case, is: *S/N* $\sim$ 14.0; this rather low value is justified by the anomalous excess of noise as pointed out before.

- The response function (fig. 7) is symmetric, and the component due to the two-strip clusters is spread between the two peaks, while the rest is mainly due to one-strip clusters.

So we conclude that the detector seems to work well in the fully depleted region even after the irradiation procedure.

Now we study the behaviour of several quantities as a function of the temperature and V_{bias} scan.

4.2 Signal/Noise

In fig. 8 the cluster noise is plotted as a function of V_{bias} at different temperatures.

Increasing V_{bias} the noise decreases slightly, due to the progressive overdepletion of the sensor.

In fig. 9 we see the same data plotted as a function of the temperature for several values of V_{bias}; unexpectedly we notice that the noise slightly decreases with the temperature, for all V_{bias} applied. A possible explanation for this is to be found in the dependence of the transconductance of the preamplifiers from the temperature; in fact g_m increases when the temperature decreases, hence the gain has the same behaviour and the noise too. This is confirmed by some laboratory tests carried out on unbonded hybrids. Further work is going on to calibrate the gain of each channel of the PREMUX128 chips.

On the other hand the cluster charge (the signal) grows (fig. 10) with V_{bias}, due to the increased capacity of collecting the electrons produced by the ionizing particle that traverse the silicon, while it decreases as a function of the temperature (fig. 11), due to both the same effect on the gain described for the noise and also to the temperature dependence of the electron mobility; according to several models [11], the mobility from -10 ^oC to +20 ^oC decreases, for both electron and holes, of $\sim 20\%$, causing the reshaping in time of the current signal induced by the drift of the hole-electron pairs, and hence a reduction of the charge measured during the sampling.

As a net result the signal/noise ratio (fig. 12) is increasing with V_{bias} and decreasing with the temperature (fig. 13). We do observe that when the detector is fully depleted, for the temperatures below $+5$ ^oC, the values of S/N is always bigger than 12.

We also checked that the cluster charge does not depend on the predicted interstrip position (fig.14).

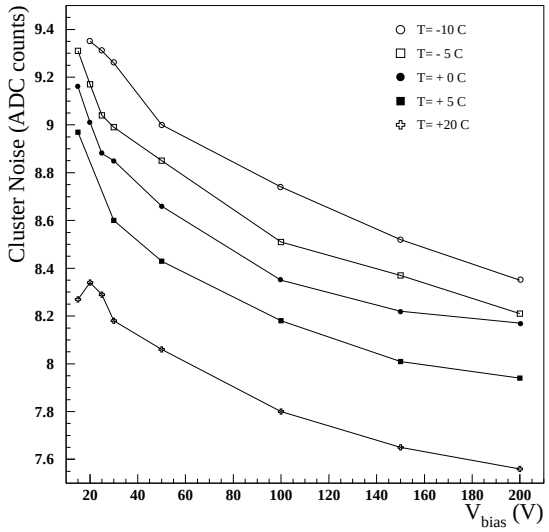

Figure 8: Cluster noise as a function of V_{bias} at various Temperature values.

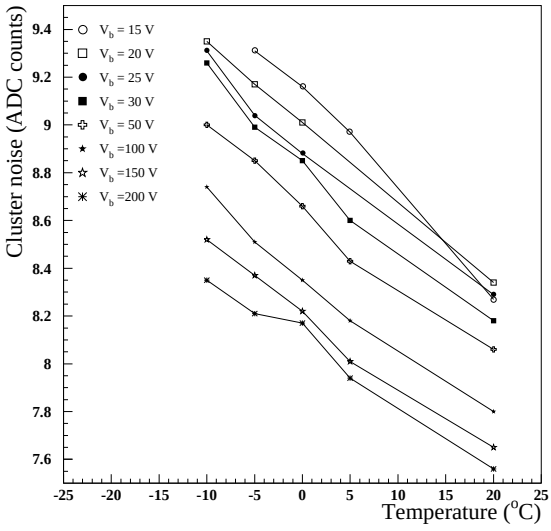

Figure 9: Cluster noise as a function of Temperature at various V_{bias} values.

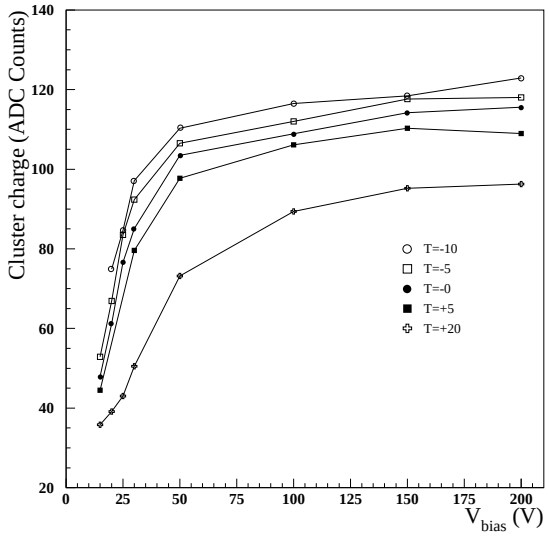

Figure 10: Cluster charge as a function of V_{bias} at various Temperature values.

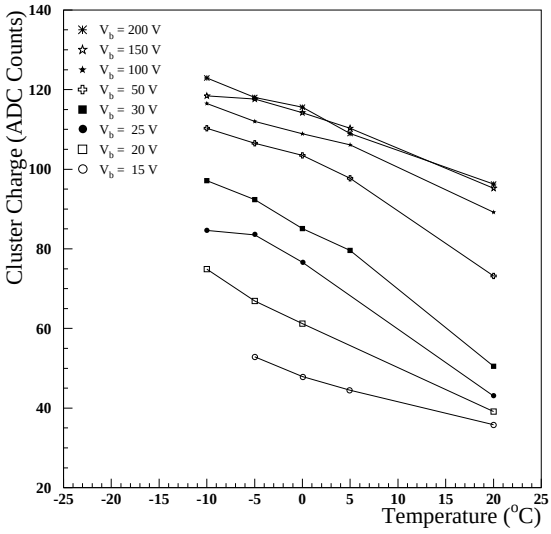

Figure 11: Cluster charge as a function of Temperature at various V_{bias} values.

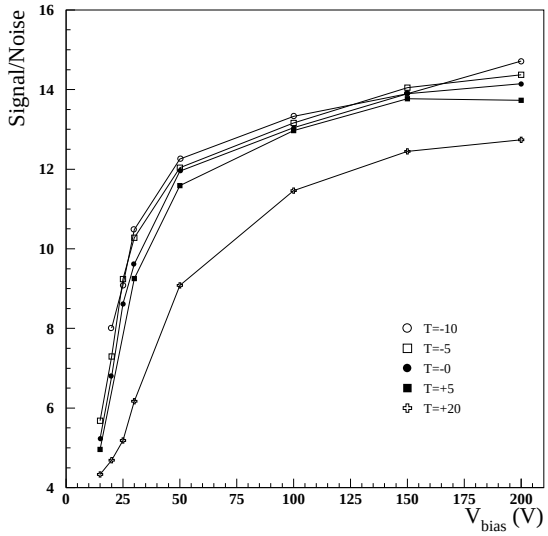

Figure 12: Signal/Noise as a function of V_{bias} at various Temperature values.

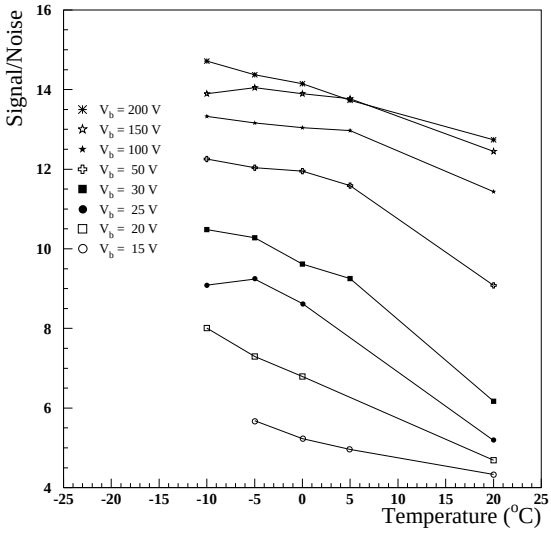

Figure 13: Signal/Noise as a function of Temperature at various V_{bias} values.

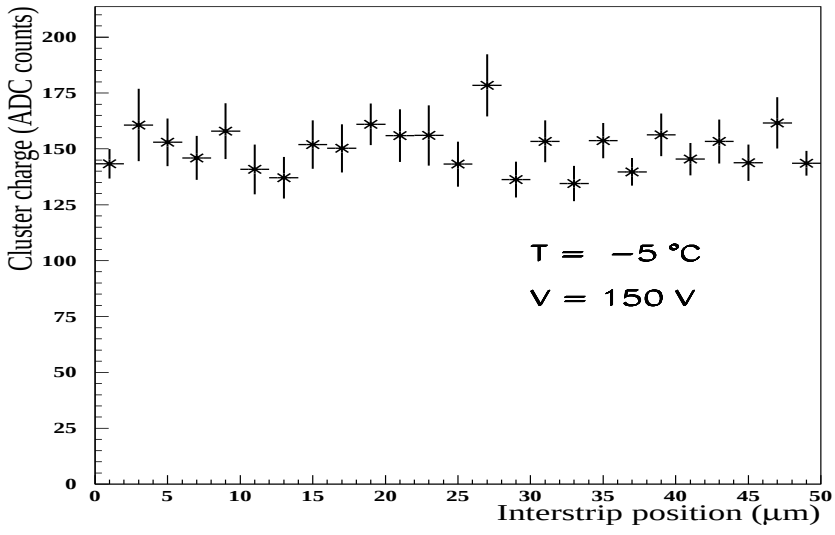

Figure 14: Average cluster charge as a function of the interstrip extrapolated coordinate.

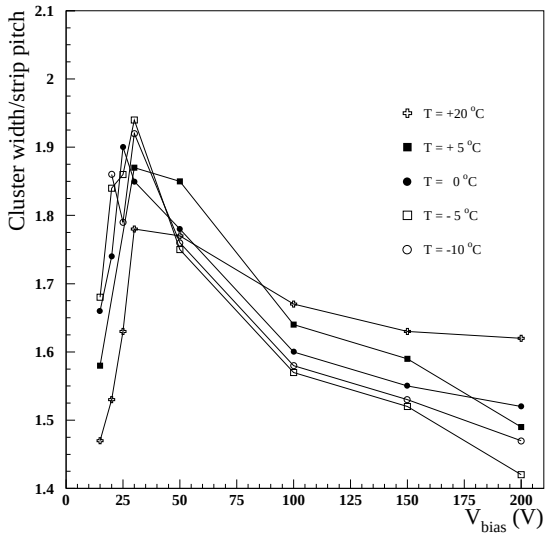

Figure 15: Cluster width.

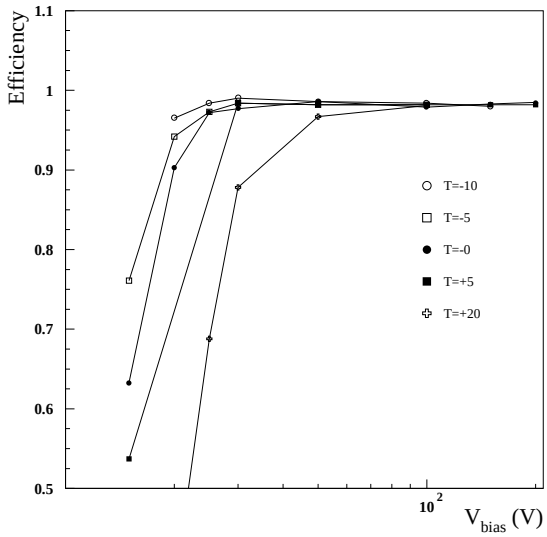

Figure 16: Efficiency as a function of V_{bias} at various Temperatures

4.3 Cluster Width

In fig. 15 we can see that the cluster width is increasing with V_{bias} at the beginning, when the detector is not yet fully depleted, it reaches a maximum around the depletion voltage (V_d = 30 V) and then decreases due to the increasing electric field inside the silicon that causes a faster drift with a corresponding reduced lateral diffusion.

Concerning the temperature dependence we observe two different behaviours: after the depletion, when the temperature is high, the width of the cluster is higher due to the increased diffusion coefficient of the electrons in the silicon. Before we reach the depletion we have the opposite behaviour, due to the fact that at low V_{bias} the sensor is not yet fully depleted and for higher temperatures the collected charge is lower, reducing the possibility for lateral strips to go over the threshold we defined in table 1.

4.4 Efficiency

To compute the efficiency we require that, to have a match with the extrapolated track from the telescope, we have to find a cluster in a fiducial region of $\pm$ 200 μm from the predicted position of the hit on the sensor. Then the efficiency is defined as ($number\ of\ matches/number\ of\ events$).

In fig. 16 we report the efficiency as a function of V_{bias} and temperature. We conclude that the sensor goes quickly at full efficiency after it is fully depleted for all the range of temperatures explored. The average efficiency is greater than 98% .

4.5 Spatial resolution

In order to study the spatial resolution we use, at the beginning, the same set of parameters (second row of table 1) used until now. First we checked that the residuals distribution is stable during the data taking; in figg. 17a-b are plotted, respectively, the residual and the average residual, computed every 200 events, versus the event number. We observe that the fluctuations of the average are within $\pm$ 7 μm and that they do not present any visible time-dependent structure.

The intrinsic resolution can be then evaluated from the width of the gaussian fit to the distribution of the residuals, subtracting in quadrature the contributions due to the extrapolation error and to the multiple scattering ($\sim$2.6 μm). In fig. 18 are reported the results as a function of V_{bias} and temperature. Essentially we can see that after the detector is fully depleted, the average value is 11.5 ± 0.5 μm. We note also that the spatial resolution shows a

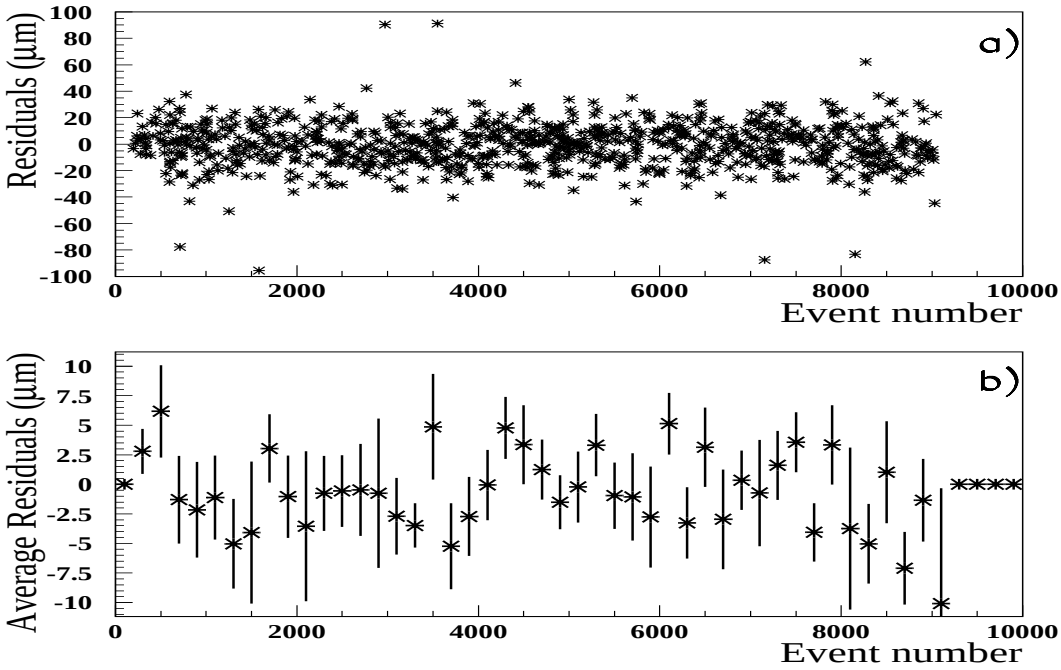

Figure 17: Stability of the residuals distribution as a function of the event number.

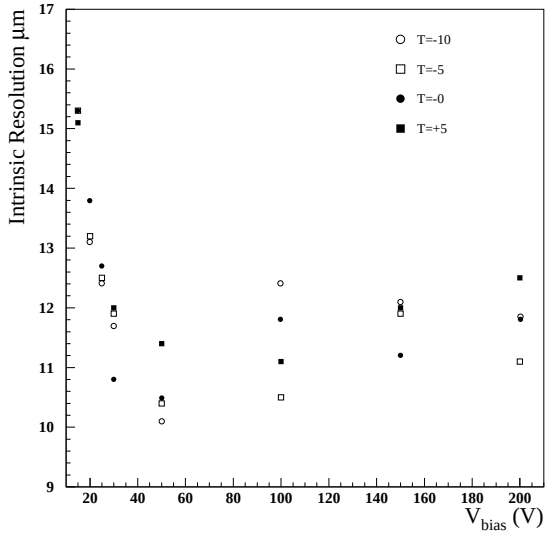

Figure 18: Spatial Resolution as a function of V_{bias} at various Temperature values.

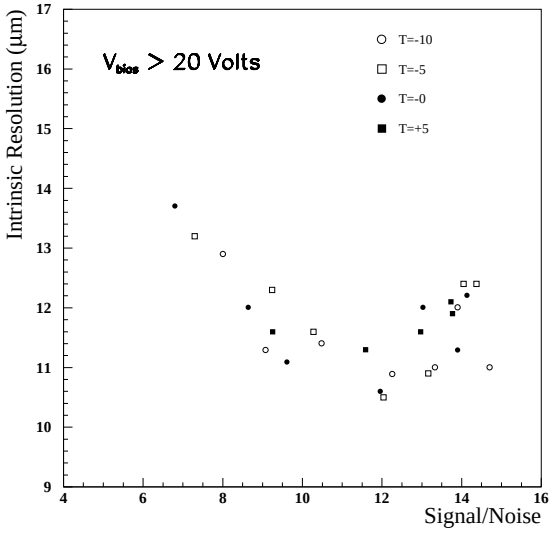

Figure 19: Signal/Noise vs Spatial Resolution for all the scan points with $V_{bias} \geq$ 15 V and T $\leq 5\ ^{o}C$.

small minimum (V_{bias}= $30 - 50\ V$) that is just after the maximum in the cluster width distribution of fig. 15, and corresponds to the region (fig. 1) where the leakage current changes the slope.

In order to check this behaviour we have used different sets of parameters to define a cluster, and we still observe the same dependence from V_{bias}, being the only difference a generalized improved (or worsened) spatial resolution of $\sim 0.5\ \mu$m.

Concerning the dependence of the resolution from the S/N we observe (fig. 19) that plotting every point of the scan with $V_{bias} \geq$ 20 V and T $\leq$ +5 ^oC, we have that for $S/N \geq 8.0$ the spatial resolution is always better than 13 μm, with an efficiency of $\sim$ 98-99 $\%$.

5 Conclusions

We have tested a single-sided silicon detector irradiated with 1×10^{13} neutrons/cm^2. We have found that the main working characteristics are still acceptable, even in presence of a noise greater than expected. In particular, if the detector is fully depleted, the signal/noise ratio is of the order of $\sim$ 12-15, the efficiency is 98-99 $\%$ and the spatial resolution is $\sim$ 10-12 μm in all investigated temperature range.

References

[1] *CMS Technical Proposal.*, **CERN/LHCC 94-38 LHCC/P1**.

[2] *Gamma and neutron irradiation facilities at ENEA - Casaccia Center (Roma)* , S. Baccaro, A. Festinesi, B. Borgia. **CMS TN/95 - 192** .

[3] *Temperature Effects on radiation Damage to Silicon Detectors* , E. Barberis et al. **Nucl. Instr. and Meth. A326: 373-380, 1993**.

[4] *Bulk Radiation Damage in Silicon Detectors and Implications for LHC Experiments*, J. Matthews et al. **Nucl. Instr. and Meth. A381: 338-348, 1996**.

[5] *Study of operating condition of semiconductors for calorimetry in LHC/SSC radiation environment*, E. Borchi et al. **Nucl. Phys. Proc. Suppl. 23B: 352-355, 1991** .

[6] *PreMux128 User Manual*, L.Jones

[7] *Signal-to-noise Evaluation for the CMS Silicon Microstrip Detectors.* C. Bozzi **CMS Note 1997/026** .

[8] *A High Resolution Beam Telescope Built with Double Sided Silicon Strip Detectors.* L. Celano et al. **Nucl. Instr. and Meth. A381: 49-56, 1996** .

[9] *Beam Test results for single and double-sided silicon detector prototypes of the CMS Central Detector.* O. Adriani et al. **Nucl. Instr. and Meth. A396 76-92 (1997)** .

[10] *Test beam results from prototypes of the upgraded Aleph vertex detector.* P. Coyle et al. **ALEPH Note 94-069** .

[11] *Analysis and simulation of semiconductor devices.* S. Selberhern **Springer Verlag** .